Speculative Streaming: Fast LLM Inference without Auxiliary Models

Nikhil Bhendawade Irina Belousova Qichen Fu Henry Mason
Mohammad Rastegari[*] **Mahyar Najibi**
Apple
{nbhendawade, ibelousova, qfu22, hmason, mrastegari, najibi}@apple.com

Abstract

Speculative decoding is a prominent technique to accelerate large language model inference by leveraging predictions from an auxiliary draft model. While effective, in application-specific settings, it often involves fine-tuning both draft and target models to achieve high acceptance rates. As the number of downstream tasks grows, draft models add significant complexity to inference systems. Recently several single model architectures viz. Medusa have been proposed to speculate tokens in non-autoregressive manner, however, their effectiveness is limited due to lack of dependency between speculated tokens. We introduce a novel speculative decoding method that integrates drafting within the target model by using Multi-stream attention and incorporates future token planning into supervised fine-tuning objective. To the best of our knowledge, this is the first parameter-efficient approach that scales well with an increasing number of downstream tasks while enhancing downstream metrics and achieving high acceptance rates, attributable to the interdependence among the speculated tokens. Speculative Streaming speeds up decoding by 1.9 - 3X in a diverse set of tasks, such as Summarization, Structured Queries, and Meaning Representation, while improving generation quality and using $\sim$10000X fewer extra parameters than alternative architectures, making it ideal for resource-constrained devices. Our approach can also be effectively deployed in lossless settings for generic chatbot applications that do not necessitate supervised fine-tuning. In such setups, we achieve 2.9 - 3.2X speedup while maintaining the integrity of the base model's output.

1 Introduction

Large transformers are today's preeminent tool for language modeling. The quality of these models improves as they scale [18], leading to the introduction of the state-of-the-art multi-billion parameter models [3, 26, 9, 28]. While these models are effective for token generation, they incur a high inference cost as the model and its transient states need to be loaded into computing memory for each subsequently generated token. This poses a challenge to the deployment of large autoregressive transformers, particularly for user-facing applications with stringent latency requirements.

Given the memory-bound nature of large language model (LLM) inference, recent work [19, 6] proposed Speculative Decoding as an effective technique to accelerate decoding based on concepts borrowed from speculative computation [4] to exploit the available extra compute. The core of speculative decoding is the idea of speculating multiple candidate future tokens first, and then verifying them all in parallel. To achieve this, as shown in Figure 1a.(i), a two-model paradigm approach is used: a small auxiliary "draft" model for candidate speculation and a large "target" model for verification [19, 6]. Although effective in accelerating LLMs, speculative decoding complicates

[*]Work done while at Apple.

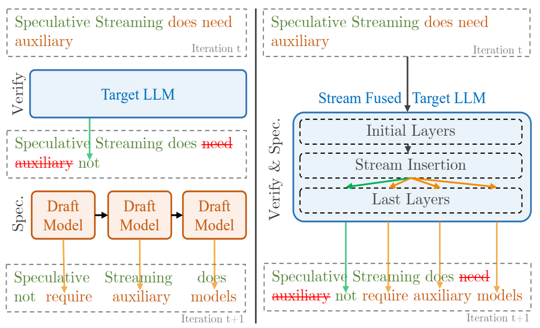
Speculative Streaming does need auxiliary
Iteration t
Verify
Target LLM
Speculative Streaming does ~~need auxiliary~~ not
Spec.
Draft Model
Draft Model
Draft Model
Speculative Streaming does not require auxiliary models
Iteration t+1
Speculative Streaming does need auxiliary
Iteration t
Stream Fused Target LLM
Verify & Spec.
Initial Layers
Stream Insertion
Last Layers
Speculative Streaming does ~~need auxiliary~~ not require auxiliary models
Iteration t+1

(a) Speculative Decoding (b) Speculative Streaming

(a) (i). Speculative Decoding requires a well-aligned draft model that runs autoregressive speculation. (ii). Speculative Streaming significantly simplifies the system by performing speculation and verification concurrently, within a single stream-fused model.

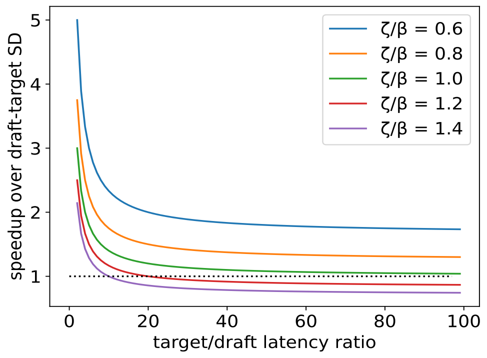

(b) Theoretical speedups of Speculative Streaming compared to draft-based speculative decoding for various ζ/β and target-to-draft latency ratios, where ζ and β represent the advancement per step for speculative decoding and Speculative Streaming, respectively.

Figure 1: Speculative Decoding vs Speculative Streaming

deployment. Training also becomes more demanding and complicated, as a separate draft model needs to be trained and aligned with the target model for each application. It is also not resource-efficient, requiring to host two models in memory during token prediction.

In this paper, we propose *Speculative Streaming*, a single-model speculative decoding approach that unifies speculation and verification, obviating the need for a separate draft model as shown in Figure 1a.(ii). This is accomplished by incorporating multi-stream attention into the target model to perform n-gram prediction which serves as future candidate speculation. As a result, a forward model pass can verify the previously generated tokens while simultaneously speculating on the future tokens. Figure 1b illustrates the theoretical speedups of our approach, demonstrating that achieving token advancement per step close to that of draft-based speculative decoding ($\zeta/\beta \approx 1$) results in greater speedups compared to conventional speculative decoding across a range of target-to-draft latency ratios.

While significantly simplifying training and inference architecture and enhancing resource efficiency, Speculative Streaming not only improves generation quality across a wide range of downstream tasks but also outperforms two-model speculative decoding [19] and other methods such as Medusa [5], Lookahead decoding [14], Hydra [34], and Eagle [33] in terms of decoding speedup. The key advantages of Speculative Streaming are as follows:

– Achieves substantial decoding speedups and improves downstream performance metrics through a single, streamlined fine-tuning process leveraging multi-stream attention.
– Demonstrates resource efficiency with significantly fewer additional parameters compared to Medusa [5], Hydra [34] and Eagle [33], while still surpassing them in speedup gains.
– Simplifies deployment by removing the complexity of managing, aligning, and switching between multiple models during inference, as required by approaches like [19].

2 Related Works

The original speculative decoding approach [6, 19] utilizes a smaller draft model to generate a candidate sequence of tokens to be verified by the *target model*. Recent SD variants propose parallel computation along the batch axis [25], and tree-structured batches [20, 22] to improve the acceptance rates of the guessed tokens by the target model and to further boost the performance. However, these methods encounter a common limitation: the necessity of developing an accurate and independent draft model for each downstream application. First, training such a draft model aligned with the main model is not trivial [38]. Second, hosting two different models increases the system complexity, and is more computationally and operationally expensive to maintain as number of applications grow.

Recently, single-model speculation has also been considered. In particular, inspired by [21, 23], Medusa [5] extends the main model to predict future tokens in parallel by training multiple output heads. While it does not require a draft model, each Medusa head of size (*hidden_size* $\times$ *vocab_size*) requires significant nonnegotiable additional parameters which introduce deployment challenges on resource-constrained devices. Furthermore dependency between speculated tokens is not guranteed [34] limiting speedups. [34] improves speculation procedure of [5] by using autoregressive draft head to introduce dependency between speculated tokens, however small size draft head tends to be sub-optimal and increasing draft head size leads to similar issues as those with [19, 38]. [33] uses a dedicated layer of target model to generate speculation, however, speedups are limited due to auto-regressive draft generation. Moreover, using a dedicated layer leads to significant parameter overhead. Lookahead decoding [14] proposes a parallel decoding method without learning new parameters. While this approach is parameter efficient, speedups are limited as speculation procedure is not learnable.

3 Method

3.1 Motivation

Existing speculative decoding techniques often enforce a strict decoupling of the training objectives between draft and target models [19], or between draft models and auxiliary heads [5]. While this separation has been effective, we propose that these objectives are not inherently orthogonal. Instead, they can be aligned during training. Specifically, we hypothesize that, similar to the main residual stream, the model can process "speculative" residual streams which can be optimized to approximate the residual streams of future tokens, extending beyond immediate next-token prediction. By conditioning immediate next token prediction on speculative streams as well as previous context, the model gains the ability to predict upcoming tokens with a richer contextual scope. As a result, this approach mitigates the risks of overly greedy decoding, providing a more informed and contextually aware generative process.

Our goal is to develop an end-to-end trainable, single-model framework that integrates future token planning, enhances generation quality, and scales efficiently across multiple downstream applications. We propose following modifications to achieve these objectives. (a) Speculative stream design and initialization as described in Section 3.1.1 (b) Parallel speculation and verification as described in Section 3.1.2 (c) Parallel tree draft pruning, described in Section 3.1.3 and finally (d) Training objective as described in Section 3.1.4.

3.1.1 Streams Design and Initialization

Parameter efficient supervised fine-tuning [16] of decoder-only pre-trained language models involves training low-rank adapters to predict next target token y_t given context tokens $(x_1....x_m)$ and previous target tokens $(y_1..y_{<t})$ on downstream applications. Although effective, this objective generates each token greedily and lacks a sense of future token planning [21] which may lead to sub-optimal generation quality (see Section 4.1.2). To inherently embed a notion of future token planning, we modify the training objective of the target model from next token prediction to n-gram prediction using multi-stream attention. This objective facilitates proactive token planning and mitigates over-fitting to local correlations [30, 21]. Furthermore, we extend this framework by sharing the key/value cache across all streams, allowing each of the γ streams to generate speculative tokens with negligible latency overhead when the model is memory-bound. Specifically, each added stream predicts $p(y_{t+j}|y_{<t}, x)$, where $1 <= j <= \gamma$, while main stream predicts $p(y_t|y_{<t}, x)$.

We enable the main stream to attend to speculative streams, allowing it to plan its residual transformations based on anticipated future residual states by modifying the standard multi-head attention mechanism [29] as

$$M_t^{k+1} = \text{MHA}(M_t^k, M_{\leq t}^k \oplus S_{t1...\gamma}^k, M_{\leq t}^k \oplus S_{t1...\gamma}^k) \quad (1)$$

where M_t^k and S_t^k refer to main and speculative streams at time step t and layer k and $MHA(H, H, H)$ denotes attention between query HW^Q, key HW^K and value HW^V as described in [29]. On the other hand, each speculative stream j at time step t attends to previous main stream hidden states and previous speculative stream hidden states as:

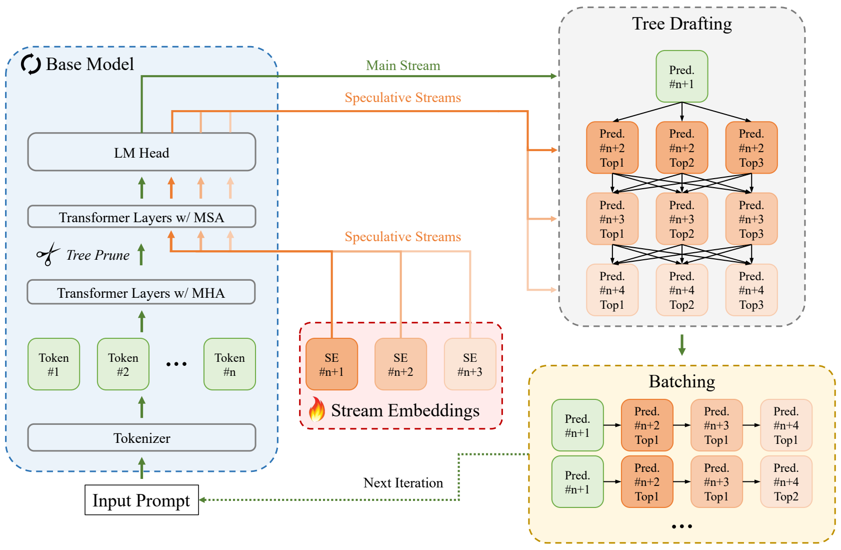

Figure 2: Architecture: We replace top N_s multi-head attention (MHA) layers of the base model with multi-stream attention (MSA) layers as described in (2). Speculative streams are initialized using hidden states of layer $N - N_s$ and stream identifier embeddings (SE), as described in (3) and used to generate speculative draft in the form of a tree. The speculative tree draft from the previous iteration is batched for verification and pruned before stream insertion. During each forward pass previous tree draft is verified and a new tree draft is issued using speculative streams as described in 3.1.2

$$S_{tj}^{k+1} = \text{MHA}(S_{tj}^k, M_{\leq t}^k \oplus S_{t(\leq j)}^k, M_{\leq t}^k \oplus S_{t(\leq j)}^k) \tag{2}$$

Hidden state of last transformer layer N, M_t^N is used to predict y_t, whereas each speculative stream at last layer, S_{tj}^N predicts y_{t+j}. We refer to layers incorporating the attention mechanism in [29] as MHA layers while layers incorporating Equation (1) and Equation (2) are referred to as MSA layers.

Key/value projections of main stream hidden states are cached during inference to avoid re-computation, whereas, we design speculative stream attention to specifically avoid storing additional key/value projections associated with individual streams. This is because speculative streams are trained to learn contextual features from main stream key/value context allowing us to not introduce additional caching overhead and operate within memory bounds of resource-constrained devices during inference. We initialize hidden states of speculative streams at layer $N - N_s$ instead of initializing them from the embedding layer, where $N_s < N$. Specifically, stream j at time t is initialized at layer $N - N_s$ as,

$$S_{tj}^{N-N_s} = f_\eta(M_t^{N-Ns}) + P_j^{N-N_s} \tag{3}$$

where P_j is a stream identifier embedding that embeds a sense of relative position into streams and distinguishes the computation from main stream. f_η is a linear transformation of rank η to transform main stream hidden states into speculative stream hidden states. This initialization helps to reduce computation per forward pass, since only the main stream needs to be passed through $N - N_s$ layers, while speculative streams are passed through the last N_s layers, decreasing the speculative FLOPs contribution by $(N - N_s)/N$ and in turn helping with peak power consumption on the device. In terms of forward pass latency, FLOPs do not contribute significantly when the model is memory bound, however, as we describe in Section 3.1.2, we sample additional tokens to make the model compute-bound, therefore FLOP reduction becomes crucial. We also experimented with value rotation based stream design which does not require identifier embeddings and incurs no parameter overhead as described in Appendix B.3.

3.1.2 Parallel Speculation and Verification

In standard draft-target speculative decoding [19], speculation and verification processes happen sequentially. Speculative Streaming makes this process efficient by parallelizing speculation and verification. In each forward pass, the draft generated in the previous step is verified and a new draft is generated as shown in Figure 2. For instance, in step s, if draft tokens $(\tilde{y_1}..\tilde{y_\delta})$ are accepted where $0 < \delta \leq \gamma$, main stream M_δ is used to issue a correction token and logits from speculative streams $S_{\delta(1...\gamma)}$ are used to generate draft for step $s+1$.

Instead of using a linear sequence of speculated tokens for verification, we sample a tree of tokens from main and speculative streams, such that each path in the tree is one possible verification candidate. Tree drafting enables accepting the longest matching candidate sequence and more tokens can be advanced during each forward pass. To create a tree draft, instead of sampling 1 token from logits of speculative streams, $(z_1...z_\gamma)$, we sample top k tokens and form a tree of sampled tokens as shown in Figure 2, such that tokens sampled from stream n are predecessors of tokens sampled from stream $n+1$. We process a tree draft of speculative tokens in one forward pass by creating an additive attention mask [29] such that each node in the tree attends to its predecessor. Attention mask between k^{th} token sampled from logits of stream j, $\tilde{y}_{jk}$ and the m^{th} token sampled from logits of stream n, $\tilde{y}_{nm}$ is

$$a_{\tilde{y}_{jk}\tilde{y}_{nm}} = \begin{cases} 0 & \text{if j = n+1,} \\ -\infty & \text{otherwise} \end{cases} \tag{4}$$

Please refer to Figure 10 for more details.

3.1.3 Parallel Tree Pruning

One of the issues with the naive creation of a speculative tree draft is that every permutation between k tokens sampled from each stream needs to be considered as a viable speculative candidate for the next verification pass. For instance, sampling k tokens from each of γ streams results in tree draft of size 1 + $\sum_{g=1}^{\gamma} k^g$. Furthermore, each of the draft tokens is batched with γ speculative streams in MSA layers to ensure that the generation of the next draft happens in the same forward pass, resulting in a batch size of $(1+\gamma) * (1 + \sum_{g=1}^{\gamma} k^g)$. As batch size increases, target model inference becomes compute-bound, obviating the latency benefit of sampling more tokens. We mitigate this problem by introducing a parallel tree draft pruning layer, which prunes less probable tokens from the input tree draft based on transition probability between parent and immediate child tokens. To obtain transition probabilities without using proxy models, we use an early-exiting-based technique. Specifically, hidden states of the main stream at layer l, M^l are passed through a low-rank linear transformation o_θ, where the rank θ is typically set to a small value like 8 to keep parameter overhead minimal. We use original language modeling head, H to obtain early exit logits, $\tilde{z} = H(o_\theta(M^l)$. $\tilde{z}_{pc}$ is used to approximate transition probability between parent token p and child token c. The pruning layer can be inserted at any point in the network, guided by the trade-off between forward pass latency and pruning accuracy. Early insertion reduces latency but risks pruning potentially valuable tokens. Conversely, late insertion retains more "good" tokens but comes at the cost of increased forward pass latency. In all experiments described in Section 4.1, we insert the pruning layer just before speculative stream insertion. More details can be found in Appendix Figure 9.

3.1.4 Training

Our supervised fine-tuning procedure entails training the base model on both the prediction loss of the next token and γ future tokens. The overall loss function is defined as follows:

$$L_{ss} = -\alpha_0(\sum_{t=1}^{T} \log p_\theta(y_t|y_{<t}, x)) - \sum_{j=1}^{\gamma} \alpha_j(\sum_{t=1}^{T-j} \log p_\theta(y_{t+j}|y_{<t}, x)) \tag{5}$$

where α_0 and α_j are set empirically to normalize losses of the next token and speculative tokens prediction using LoRA [16]. Note that adapter parameters are shared between main and speculative streams in application specific settings to increase down-stream performance. For generic chat-bot like settings where fine-tuning is not required, adapter parameters are dedicated to training of speculative streams and α_0 is set to 0. Although training with Speculative Streaming is relatively cheap (see Appendix D), naive training increases batch dimension along sequence length axis by γ

causing attention computation to hit peak memory with larger batches. We employ a segment based attention method that helps reduce peak memory consumption and increases training throughput significantly by dividing training sample into prompt and multiple completion segments. More details on segment attention can be found in Appendix C. Finally, Tree-pruning adapter described in Section 3.1.3 is trained on the next token prediction loss.

3.1.5 Acceptance Criteria

We employ rejection sampling based acceptance criteria used in [6] to avoid distribution shift from base target model. Acceptance of draft tokens from each path in pruned tree (see Section 3.1.3) is run as per rejection sampling scheme and longest accepted path is used to advance decoding. Please refer to Appendix A.1 for more details.

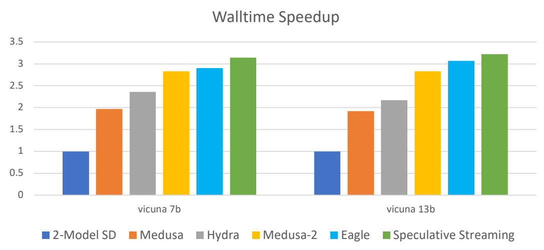

Figure 3: Walltime speedup on Vicuna models of various sizes to demonstrate scalability and generalizability of our approach on MT-Bench.

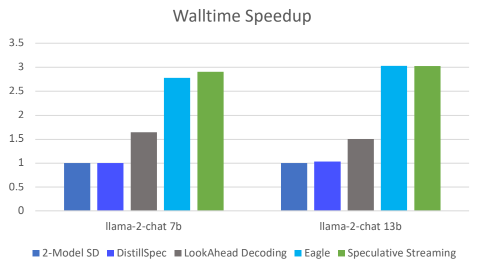

Figure 4: Walltime speedup on Llama-2 models of various sizes to demonstrate scalability and generalizability of our approach on MT-Bench.

4 Experiments

We evaluate our methods on a diverse set of downstream applications as well as generic reasoning oriented conversational tasks using pre-trained models of various scales.

Datasets. To test our method on user-facing application specific settings that are vital to on-device AI assistants we use a diverse set of tasks namely Text Summarization, Structured Queries and Meaning Representation using Dialogsum [7] dataset, the sql-create-context dataset built from WikiSQL [37] and SPIDER [32], and e2e-nlg dataset [11] respectively. Along with application specific settings, to test generalizability of our method, we evaluate on reasoning oriented chat-bot like setup using the multi-turn dialogue dataset, MT-bench [36].

Model Configuration. We tested four different open source models of various scales, Phi-3-mini-4k-instruct(3.8B)[1], Llama-2(7B)[27], Mistral(7B) [17] and OPT(1.3B, 6.7B) [35] on application specific settings. To test scalability of our approach we use Vicuna Models (7B, 13B, 33B) [8] and Llama-2 chat models (7B, 13B). We compare our method with the draft-target speculative decoding methods [19, 38] and single-model speculative decoding frameworks, Medusa [5], LookAhead decoding [14], Hydra [34] and Eagle [33]. For the standard draft-target approach, we use OPT-125m, the smallest configuration of available open-source OPT models as the draft model.

Metrics. For application specific settings, we report wall-time speedups and generation quality metrics on held-out test set. We use Exact Match (EM) accuracy metric for the structured query task and Rouge1/RougeLSum metrics for the Dialog Summarization and Meaning Representation tasks. For generic chat-bot like settings, where fine-tuning is not required, we train speculative streams while keeping base model frozen as noted in Section 3.1.4 and report speedup and inference overhead.

Inference. Inference is performed using a batch size of 1 on a single Nvidia A100-80G GPU in float16 using greedy sampling and $T = 0$. Please refer to Appendix F for batching impact, Appendix B.4 for ablations on top-k sampling, $T = 1$ and Appendix G.1 for more experimental details. We set $N_s = 4$, $\gamma = 3$ and $k = 3$ for all experiments. Please refer to Appendix for hyperparameter ablations.

Table 1: Comparison of walltime speedup, CR ratio, and parameter overhead across models of different scales fine-tuned for downstream tasks. CR ratio indicates accelerator agnostic call reduction ratio. Metrics include exact match accuracy for SqlContext and Rouge for Dialogsum and E2E-NLG. Medusa and Speculative streaming parameters are fine-tuned jointly with the base model, while the base model is frozen during Eagle fine-tuning to to prevent adverse effects on generation metrics.

Dataset	Model	Method	SpeedUp (↑)	CR Ratio (↑)	Metric (↑)	# Extra Parameters (↓)
SqlContext	Mistral-Instruct-7B	Baseline	1.00	1.00	84.16	–
		Medusa-2	2.79	3.18	84.18	$5.9E8$
		Eagle	2.75	3.58	84.16	$2.4E8$
		SS (ours)	**2.93**	**3.67**	**84.50**	$8.2E4$
	PHI-3-Instruct-3.8B	Baseline	1.00	1.00	80.92	–
		Medusa-2	2.54	2.81	81.07	$4.3E8$
		Eagle	2.62	3.37	80.92	$1.3E8$
		SS (ours)	**2.92**	**3.65**	**84.10**	$6.1E4$
	Llama2-7b	Baseline	1.00	1.00	85.37	–
		Medusa-2	2.52	2.98	85.31	$5.9E8$
		Eagle	2.59	3.31	85.37	$2.4E8$
		SS (ours)	**2.81**	**3.57**	**85.93**	$8.2E4$
DialogSum	Mistral-Instruct-7B	Baseline	1.00	1.00	44.74/36.76	–
		Medusa-2	1.89	2.05	44.78/36.95	$5.9E8$
		Eagle	1.95	2.56	44.74/36.76	$2.4E8$
		SS (ours)	**2.04**	**2.96**	**44.89/37.09**	$8.2E4$
	PHI-3-Instruct-3.8B	Baseline	1.00	1.00	46.08/38.28	–
		Medusa-2	2.15	2.26	45.82/37.78	$4.3E8$
		Eagle	2.05	2.31	46.08/38.28	$1.3E8$
		SS (ours)	**2.32**	**2.85**	**46.30/38.32**	$6.1E4$
	Llama2-7b	Baseline	1.00	1.00	44.90/37.0	–
		Medusa-2	1.76	1.95	44.17/37.02	$5.9E8$
		Eagle	1.86	2.57	44.90/37.0	$2.4E8$
		SS (ours)	**1.90**	**3.05**	**45.0/37.85**	$8.2E4$
E2E-NLG	Mistral-Instruct-7B	Baseline	1.00	1.00	67.82/48.99	–
		Medusa-2	2.78	3.19	67.74/48.85	$5.9E8$
		Eagle	2.85	3.52	67.82/48.99	$2.4E8$
		SS (ours)	**2.93**	**3.67**	**68.37/49.09**	$8.2E4$
	PHI-3-Instruct-3.8B	Baseline	1.00	1.00	68.72/49.31	–
		Medusa-2	2.39	2.63	68.41/49.08	$4.3E8$
		Eagle	**2.42**	**2.76**	68.72/49.31	$1.3E8$
		SS (ours)	2.36	2.72	**69.38/50.22**	$6.1E4$
	Llama2-7b	Baseline	1.00	1.00	69.47/49.54	–
		Medusa-2	2.82	3.19	69.41/49.44	$5.9E8$
		Eagle	2.79	3.26	69.47/49.54	$2.4E8$
		SS (ours)	**2.89**	**3.38**	**69.52/49.93**	$8.2E4$

4.1 Results

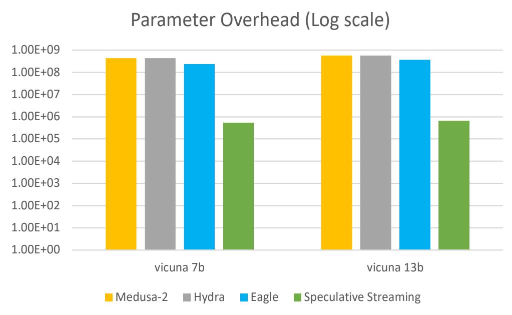

Figure 5: Parameter/Memory access overhead of different SD architectures with Vicuna models.

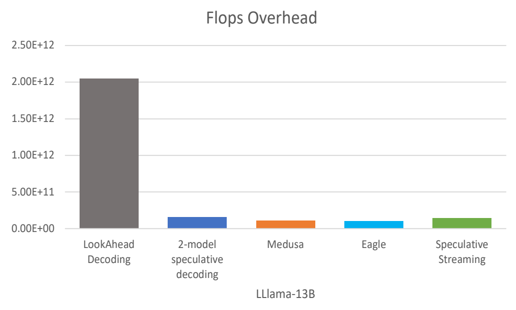

Figure 6: FLOP overhead of different SD architectures with Llama-13B.

4.1.1 Effectiveness

Table 1 presents the comparison between standard auto-regressive decoding baseline, Medusa, Eagle and our approach in terms of speedup, call reduction ratios, and the number of extra parameters. We

Table 2: Walltime latency (per sample) and auto-regressive calls comparison with standard draft-target (Two-model) speculative decoding approach using OPT-125m as the draft model.

Dataset	Target	Method	Target calls	Draft Calls	Walltime Latency (ms, ↓)	Metric (↑)
SqlContext	OPT-1.3b	Two-model SD	6.59	22.35	269.24	84.98
		SS (ours)	7.79	0	**133.48**	**87.40**
	OPT-6.7b	Two-model SD	6.60	22.41	301.10	89.13
		SS (ours)	6.88	0	**157.04**	**89.34**
Dialogsum	OPT-1.3b	Two-model SD	11.65	42.59	493.59	43.40/35.60
		SS (ours)	13.41	0	**248.26**	**44.07/35.99**
	OPT-6.7b	Two-model SD	12.15	35.76	555.99	44.40/36.60
		SS (ours)	14.45	0	**444.67**	**44.42/36.81**
E2E-NLG	OPT-1.3b	Two-model SD	8.86	31.47	345.72	**69.48**/50.17
		SS (ours)	9.80	0	**164.23**	69.32/**50.51**
	OPT-6.7b	Two-model SD	8.90	31.58	412.02	69.34/**49.88**
		SS (ours)	10.31	0	**244.80**	**69.45**/49.78

find that across a variety of downstream tasks, the walltime speedups and call reduction ratios of Speculative Streaming are consistently higher than alternatives while incurring significantly lesser parameter overhead. Furthermore, as summarized in Table 2, our approach achieves better wall-time latencies than the standard draft-target speculative decoding since the difference in the number of target calls between both approaches is not large enough to offset auto-regressive drafting overhead. Please refer to Appendix G for more insights. Finally, it is worth noting that the generation metrics of our method are consistently better than next token prediction based fine-tuning making it an excellent alternative to LoRA based next-token prediction fine-tuning. Speedup gains of our approach remain consistent in generic conversational tasks evaluated on MT-Bench. Our approach achieves better speedup than alternatives across Vicuna and Llama models of various scales (see Figure 3, Figure 4) in lossless settings while incurring significantly lesser memory access and compute overhead (see Figure 5, Figure 6) demonstrating generalizability and scalability of our approach.

4.1.2 Why Does It Work?

Generation Metrics: To investigate the improvements in generation quality achieved by our approach, we designed an experiment where the model predicts the next token while attending to a set of future γ ground truth tokens beyond the next token. Our hypothesis was that by granting the model access to these future tokens, the attention mechanism would enhance its ability to anticipate and plan for the next token, thus improving generation quality. Specifically, we postulated that:

$$p(y_t = g_t | y_{<t}, y_{t+1..t+\gamma}, x) > p(y_t = g_t | y_{<t}, x) \tag{6}$$

Here, g_t represents the ideal ground truth token that maximizes the generation quality metrics. To validate this hypothesis, we modified the attention mask, allowing the model's residual states to "peek" into future residuals. As shown in Figure 13, this modification led to significant improvements in generation metrics.

While such access to future tokens is not feasible during inference—where future states are unavailable—our approach enables the model to approximate future residual states using speculative streams. As demonstrated in Figure 12, these speculative streams, S_{tj}, progressively align with the true residual states of the next tokens as they propagate through the model layers. Crucially, our method allows the primary stream, M_t, to attend not only to the current context up to token y_t but also to the speculative streams S_{tj}. This multi-stream attention mechanism refines the transformations within M_t, aligning them more closely with the context of the upcoming γ tokens. As a result, the model effectively "plans" for future tokens, leading to measurable improvements in generation quality.

Speedup: Medusa attempts to generate the hidden states of speculative tokens $y_{(t+1...t+\gamma)}$ by applying a simple linear transformation to the last hidden state of the current token y_t. However, this method has significant limitations. The absence of attention mechanisms or non-linear transformations results in lower similarity metrics between the speculative hidden states generated by Medusa and the true hidden states, which are obtained by feeding the actual next token into the model (see Figure 12). In contrast, our proposed technique leverages multi-stream attention, wherein speculative streams are allowed to attend to each other as well as to the main stream. As these streams propagate through the model layers, they more closely approximate the true hidden states of the actual next tokens, resulting in higher similarity, thereby increasing the acceptance rate of the speculated tokens.

4.2 Ablations

We conducted extensive ablation studies to identify the optimal draft size and to evaluate the impact of tree pruning, as illustrated in Figure 7. Tree pruning enhances speedup by eliminating less probable speculative paths, thereby preventing the model from entering a compute-bound phase. Further details are provided in Appendix B. Additional ablations were performed to determine the ideal number of Multi-stream Attention (MSA) layers and their influence on fine-tuning performance, as well as the effects of value projection rotation and Top-k sampling. An increase in the number of MSA layers consistently improves generation metrics across all downstream tasks, supporting the hypothesis that Multi-Stream Attention facilitates effective planning. Our method also demonstrates robustness to non-greedy Top-k sampling, which is critical for maintaining diversity and quality control in generated text. Please refer to Appendix B for comprehensive results.

5 Conclusion

In this paper, we proposed Speculative Streaming, a method to accelerate decoding of large language models. Compared to the standard speculative decoding approaches, Speculative Streaming removes the need for an auxiliary "draft" model. Instead, it unifies speculation and verification by efficiently fusing multiple speculative streams into a single "target" model. Speculative Streaming simplifies the fine-tuning process and achieves better generation quality and speedup compared to previous approaches. It is also parameter efficient and removes the need for loading two models into the memory, making it a suitable approach for resource-constrained scenarios.

References

[1] Marah Abdin et al. Phi-3 technical report: A highly capable language model locally on your phone, 2024.

[2] Rishabh Agarwal, Nino Vieillard, Piotr Stanczyk, Sabela Ramos, Matthieu Geist, and Olivier Bachem. Gkd: Generalized knowledge distillation for auto-regressive sequence models. *arXiv preprint arXiv:2306.13649*, 2023.

[3] Tom Brown, Benjamin Mann, Nick Ryder, Melanie Subbiah, Jared D Kaplan, Prafulla Dhariwal, Arvind Neelakantan, Pranav Shyam, Girish Sastry, Amanda Askell, et al. Language models are few-shot learners. *Advances in neural information processing systems*, 33:1877–1901, 2020.

[4] F Warren Burton. Speculative computation, parallelism, and functional programming. *IEEE Transactions on Computers*, 100(12):1190–1193, 1985.

[5] Tianle Cai, Yuhong Li, Zhengyang Geng, Hongwu Peng, and Tri Dao. Medusa: Simple framework for accelerating llm generation with multiple decoding heads. `https://github.com/FasterDecoding/Medusa`, 2023.

[6] Charlie Chen, Sebastian Borgeaud, Geoffrey Irving, Jean-Baptiste Lespiau, Laurent Sifre, and John Jumper. Accelerating large language model decoding with speculative sampling. *arXiv preprint arXiv:2302.01318*, 2023.

[7] Yulong Chen, Yang Liu, Liang Chen, and Yue Zhang. DialogSum: A real-life scenario dialogue summarization dataset. In Chengqing Zong, Fei Xia, Wenjie Li, and Roberto Navigli, editors, *Findings of the Association for Computational Linguistics: ACL-IJCNLP 2021*, pages 5062–5074, Online, August 2021. Association for Computational Linguistics.

[8] Wei-Lin Chiang, Zhuohan Li, Zi Lin, Ying Sheng, Zhanghao Wu, Hao Zhang, Lianmin Zheng, Siyuan Zhuang, Yonghao Zhuang, Joseph E. Gonzalez, Ion Stoica, and Eric P. Xing. Vicuna: An open-source chatbot impressing gpt-4 with 90%* chatgpt quality, March 2023.

[9] Aakanksha Chowdhery, Sharan Narang, Jacob Devlin, Maarten Bosma, Gaurav Mishra, Adam Roberts, Paul Barham, Hyung Won Chung, Charles Sutton, Sebastian Gehrmann, et al. Palm: Scaling language modeling with pathways. *Journal of Machine Learning Research*, 24(240):1–113, 2023.

[10] Tim Dettmers, Ruslan Svirschevski, Vage Egiazarian, Denis Kuznedelev, Elias Frantar, Saleh Ashkboos, Alexander Borzunov, Torsten Hoefler, and Dan Alistarh. Spqr: A sparse-quantized representation for near-lossless llm weight compression. *arXiv preprint arXiv:2306.03078*, 2023.

[11] Ondřej Dušek, Jekaterina Novikova, and Verena Rieser. Evaluating the State-of-the-Art of End-to-End Natural Language Generation: The E2E NLG Challenge. *Computer Speech & Language*, 59:123–156, January 2020.

[12] Elias Frantar and Dan Alistarh. Sparsegpt: Massive language models can be accurately pruned in one-shot. In *International Conference on Machine Learning*, pages 10323–10337. PMLR, 2023.

[13] Elias Frantar, Saleh Ashkboos, Torsten Hoefler, and Dan Alistarh. Gptq: Accurate post-training quantization for generative pre-trained transformers. *arXiv preprint arXiv:2210.17323*, 2022.

[14] Yichao Fu, Peter Bailis, Ion Stoica, and Hao Zhang. Breaking the sequential dependency of llm inference using lookahead decoding, November 2023.

[15] Yuxian Gu, Li Dong, Furu Wei, and Minlie Huang. Knowledge distillation of large language models. *arXiv preprint arXiv:2306.08543*, 2023.

[16] Edward J Hu, Yelong Shen, Phillip Wallis, Zeyuan Allen-Zhu, Yuanzhi Li, Shean Wang, Lu Wang, and Weizhu Chen. LoRA: Low-rank adaptation of large language models. In *International Conference on Learning Representations*, 2022.

[17] Albert Q. Jiang et al. Mistral 7b, 2023.

[18] Jared Kaplan, Sam McCandlish, Tom Henighan, Tom B Brown, Benjamin Chess, Rewon Child, Scott Gray, Alec Radford, Jeffrey Wu, and Dario Amodei. Scaling laws for neural language models. *arXiv preprint arXiv:2001.08361*, 2020.

[19] Yaniv Leviathan, Matan Kalman, and Yossi Matias. Fast inference from transformers via speculative decoding. In *International Conference on Machine Learning*, pages 19274–19286. PMLR, 2023.

[20] Xupeng Miao, Gabriele Oliaro, Zhihao Zhang, Xinhao Cheng, Zeyu Wang, Rae Ying Yee Wong, Zhuoming Chen, Daiyaan Arfeen, Reyna Abhyankar, and Zhihao Jia. Specinfer: Accelerating generative llm serving with speculative inference and token tree verification. *arXiv preprint arXiv:2305.09781*, 2023.

[21] Weizhen Qi, Yu Yan, Yeyun Gong, Dayiheng Liu, Nan Duan, Jiusheng Chen, Ruofei Zhang, and Ming Zhou. Prophetnet: Predicting future n-gram for sequence-to-sequence pre-training. *arXiv preprint arXiv:2001.04063*, 2020.

[22] Benjamin Spector and Chris Re. Accelerating llm inference with staged speculative decoding. *arXiv preprint arXiv:2308.04623*, 2023.

[23] Mitchell Stern, Noam Shazeer, and Jakob Uszkoreit. Blockwise parallel decoding for deep autoregressive models. *Advances in Neural Information Processing Systems*, 31, 2018.

[24] Mingjie Sun, Zhuang Liu, Anna Bair, and J Zico Kolter. A simple and effective pruning approach for large language models. *arXiv preprint arXiv:2306.11695*, 2023.

[25] Ziteng Sun, Ananda Theertha Suresh, Jae Hun Ro, Ahmad Beirami, Himanshu Jain, and Felix Yu. Spectr: Fast speculative decoding via optimal transport. *arXiv preprint arXiv:2310.15141*, 2023.

[26] Romal Thoppilan, Daniel De Freitas, Jamie Hall, Noam Shazeer, Apoorv Kulshreshtha, Heng-Tze Cheng, Alicia Jin, Taylor Bos, Leslie Baker, Yu Du, et al. Lamda: Language models for dialog applications. *arXiv preprint arXiv:2201.08239*, 2022.

[27] Hugo Touvron et al. Llama 2: Open foundation and fine-tuned chat models, 2023.

[28] Hugo Touvron, Thibaut Lavril, Gautier Izacard, Xavier Martinet, Marie-Anne Lachaux, Timothée Lacroix, Baptiste Rozière, Naman Goyal, Eric Hambro, Faisal Azhar, et al. Llama: Open and efficient foundation language models. *arXiv preprint arXiv:2302.13971*, 2023.

[29] Ashish Vaswani, Noam Shazeer, Niki Parmar, Jakob Uszkoreit, Llion Jones, Aidan N Gomez, Łukasz Kaiser, and Illia Polosukhin. Attention is all you need. *Advances in neural information processing systems*, 30, 2017.

[30] Zhilin Yang, Zihang Dai, Yiming Yang, Jaime Carbonell, Russ R Salakhutdinov, and Quoc V Le. Xlnet: Generalized autoregressive pretraining for language understanding. *Advances in neural information processing systems*, 32, 2019.

[31] Zhewei Yao, Reza Yazdani Aminabadi, Minjia Zhang, Xiaoxia Wu, Conglong Li, and Yuxiong He. Zeroquant: Efficient and affordable post-training quantization for large-scale transformers. *Advances in Neural Information Processing Systems*, 35:27168–27183, 2022.

[32] Tao Yu, Rui Zhang, Kai Yang, Michihiro Yasunaga, Dongxu Wang, Zifan Li, James Ma, Irene Li, Qingning Yao, Shanelle Roman, et al. Spider: A large-scale human-labeled dataset for complex and cross-domain semantic parsing and text-to-sql task. *arXiv preprint arXiv:1809.08887*, 2018.

[33] Chao Zhang Hongyang Zhang Yuhui Li, Fangyun Wei. Eagle: Speculative sampling requires rethinking feature uncertainty, 2024.

[34] Aniruddha Nrusimha Christopher Rinard Jonathan Ragan-Kelley William Brandon Zachary Ankner, Rishab Parthasarathy. Hydra: Sequentially-dependent draft heads for medusa de- coding, 2024.

[35] Susan Zhang, Stephen Roller, Naman Goyal, Mikel Artetxe, Moya Chen, Shuohui Chen, Christopher Dewan, Mona Diab, Xian Li, Xi Victoria Lin, et al. Opt: Open pre-trained transformer language models. *arXiv preprint arXiv:2205.01068*, 2022.

[36] Lianmin Zheng, Wei-Lin Chiang, Ying Sheng, Siyuan Zhuang, Zhanghao Wu, Yonghao Zhuang, Zi Lin, Zhuohan Li, Dacheng Li, Eric. P Xing, Hao Zhang, Joseph E. Gonzalez, and Ion Stoica. Judging llm-as-a-judge with mt-bench and chatbot arena, 2023.

[37] Victor Zhong, Caiming Xiong, and Richard Socher. Seq2sql: Generating structured queries from natural language using reinforcement learning. *CoRR*, abs/1709.00103, 2017.

[38] Yongchao Zhou, Kaifeng Lyu, Ankit Singh Rawat, Aditya Krishna Menon, Afshin Rostamizadeh, Sanjiv Kumar, Jean-François Kagy, and Rishabh Agarwal. Distillspec: Improving speculative decoding via knowledge distillation. *arXiv preprint arXiv:2310.08461*, 2023.

A Implementation Details

A.1 Acceptance Criteria

Acceptance of draft tokens from each path in pruned tree (Section 3.1.3) is run as per rejection sampling scheme and longest accepted path is used to advance decoding. To conform to rejection sampling, we replace draft model distribution with virtual distribution that uses prophet streams. Specifically, we replace $p(x|(x_1..x_{n+t-1}))$ in algorithm 2 in [6] with $q(x|(x_1..x_n, s_{n0}..s_{n(t-1)}))$ so our acceptance criteria becomes

$$r < \min\left(1, \left\{\frac{q(x|(x_1,\ldots,x_{n+t-1}))}{q(x|(x_1,\ldots,x_n,s_{n0},\ldots,s_{n(t-1)}))}\right\}\right) \tag{7}$$

where p and q denote draft and target distributions in [6], $r \sim U[0,1]$ and $1 <= t <= \gamma$. We sample correction as

$$x_{n+t} \sim q(x \mid (x_1,\ldots,x_{n+t-1})) - q(x \mid (x_1,\ldots,x_n,s_{n0},\ldots,s_{n(t-1)})) \tag{8}$$

A.2 Tree Draft Management

In this section, we go into more detail of tree draft sampling, flattening, and pruning. As shown in the main paper, when processing prompt $(x_1...x_t)$, we insert speculative streams along with the last token to generate logits, z_t corresponding to main stream and $(z_{t1}...z_{t\gamma})$ corresponding to speculative streams. Tree draft is sampled following the procedure described in Section 3.1.2. The sampled draft is then flattened along the sequence length dimension and the attention mask is composed such that child nodes attend to their predecessors starting with root as shown in Figure 9 and Figure 10. The root token of the tree draft is the correction issued by main stream. Each iteration after prompt processing involves verifying the previous tree draft and sampling a new one. After passing the tree draft through $N - N_s$ layers, we use contextual features learned by middle layers to approximate transition probability between parent and child tokens. As shown in Figure 9, since the transition probability between token "$parameter''$ and "$compare''$ is less than a set threshold, we prune the sub-tree starting from "$compare$" in the feature domain , and m_2, m_5, m_6 are pruned. Please note that the key value cache of layers $0..(N - N_s - 1)$ before the pruning layer is not trimmed at this point to keep pruning latency overhead minimal. Key value cache backtracking is done lazily after each generation step. Speculative streams are inserted alongside each node in the pruned draft. Layers $(N - N_s..N)$ use Multi-stream attention as described in Equation (1) and Equation (2). The verification procedure finds the longest matching path in the pruned tree that main stream can accept. As shown in Figure 9, path ("$parameter''$, "$efficient''$, "$speculative''$) is accepted. Correction token sampled from logits of main stream corresponding to last accepted token, m_1 becomes new root while tokens sampled from logits of streams (s_{10}, s_{11}) form the sub-tree.

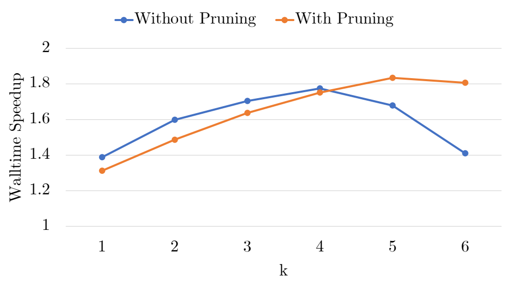

Figure 7: As more tokens (k) are sampled for tree drafting, speedup initially increases. This trend reverses as k continues to increase as the model transits to the compute-bound phase. Pruning less probable paths helps reduce compute, offering more speedup.

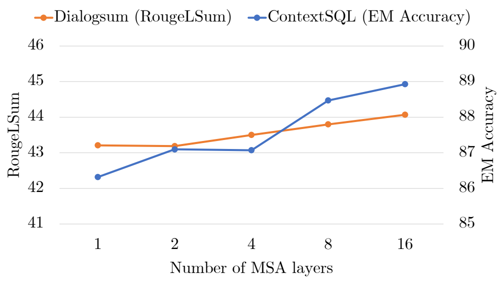

Figure 8: As the number of multi-stream attention layers increases, metrics on downstream tasks improves.

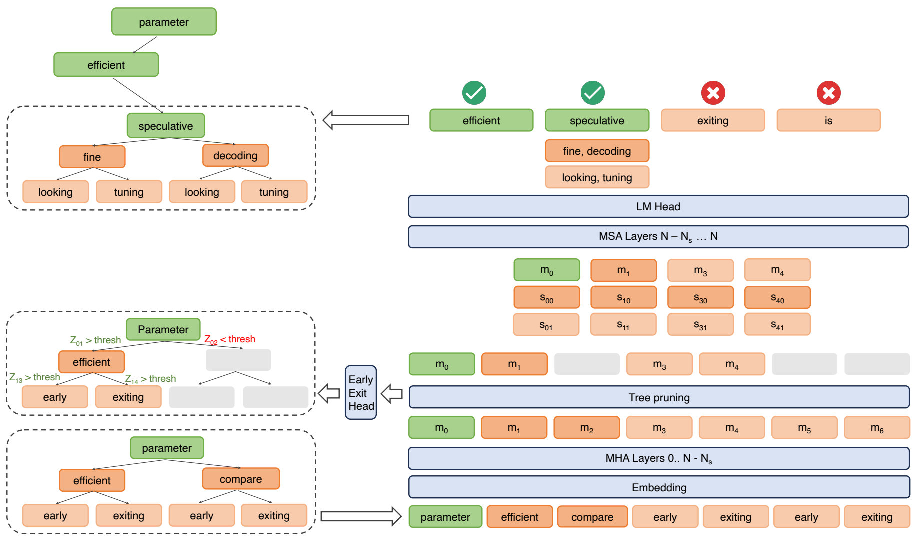

Figure 9: Parallel tree draft speculation and verification: Tree draft from the previous iteration is flattened for verification. After $N - N_s$ MHA layers, the tree pruning procedure obviates less probable tokens based on transition probability between parent and child tokens. In this illustration Z_i denotes normalized early exit logits corresponding to main stream at index i, m_i, while Z_{ij} denotes transition probability between token at index i and j in flattened tree draft. The verification procedure is subsequently run on the pruned tree and speculative tokens are sampled from streams corresponding to the latest accepted token. In above illustration, "$speculative''$", "$fine, decoding''$" and "$looking, tuning''$" are sampled from streams m_1, s_{10} and s_{11}.

B Ablation:

B.1 Speculative Draft Size.

To improve the acceptance rate of the tree draft, we try various settings of γ, the number of speculative positions, and k, the number of sampled tokens per speculative position. Figure 7 shows walltime speedup for $\gamma = 3$. As we sample more tokens from each speculative position, advancement per forward pass, β increases since more candidates are available for verification, leading to more speedup. However, as we continue to increase k, forward pass latency overhead becomes more prevalent as the model transitions into compute-bound phase and the speedup reverses the course. This is because naively forming a tree draft leads to an exponential increase in batch size with k as described in 3.1.3. We insert a tree pruning layer to remove less probable paths and reduce the size of the tree draft. Pruning tree draft reduces forward pass latency, and a well calibrated threshold ensures that only noisy paths in the tree get pruned. Tree pruning tends to help with walltime speedup as k continues to increase as shown in Figure 7.

B.2 Number of MSA Layers

There are trade-offs involved in deciding the number of MSA layers to incorporate in terms of downstream generation metric, training time, and FLOPs increase. As we increase the number of MSA layers, the generation metric improves and this trend remains the same across different downstream tasks. Typically incorporating MSA in the top 2 - 8 layers offers a good trade-off between metric, FLOPs increase and training time. Figure 8 shows the generation performance of the OPT-1.3b model on Structured Query and Summarization tasks.

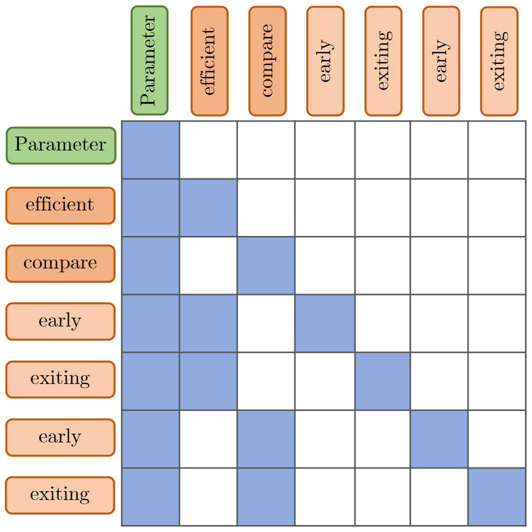

Figure 10: Attention mask for tree draft is composed in such a way that child tokens can attend to all predecessors starting from root, root being correction issued by main stream. In this illustration, "$early$" attends to "$parameter$" and "$efficient$" and itself since "$parameter-efficient-early$" forms one path in tree. "$early$" is also replicated to form another path "$parameter - compare - early$". This attention mask allows batching multiple paths and increasing acceptance rate as number of candidates increase.

B.3 Value Rotation

We analyzed more ways of differing computation of main stream from speculative streams. Apart from using dedicated stream embeddings, one way to differentiate the computation while incorporating a sense of relative position is simply rotating streams relative to each other. In this ablation, we initialize each stream with the main stream hidden state and rotate the value projection during attention computation in the proportion of the relative distance from main stream as :

$$V_{tn}^{k} = V_{t}^{k} e^{i\epsilon n} \tag{9}$$

Where $1 <= n <= \gamma$ is stream index, V_t^k denotes value projection of main stream at time step t and layer k, while V_{tn}^k denotes value projection of stream n, $0 \leq \epsilon \leq \frac{\pi}{2N}$ denotes an arbitrary rotation step and N denotes the sum of maximum sequence length and number of streams. Figure 11 (a) shows the effect of using value rotation on Rouge scores on the Dialog Summarization task with the Phi-1.3b model. Downstream metric for value rotation-based approach tends to be lower than using dedicated stream embeddings across different settings of MSA layers, however, the trend of increasing metric with added MSA layers remains the same. It is worth noting that for $N_s = 16$, simply rotating value projections achieve better metrics than using $N_s = 4$ with dedicated stream embeddings.

B.4 Top-k Sampling

In the main paper, we reported speedup results using greedy sampling and T=0. To further analyze speedups in the Top-k sampling regime, we try various values of k and T = 1 for both Medusa style and Speculative Streaming approaches. Figure 11 (b) shows the effect of increasing k on the walltime speedups and call reduction ratios. Although increasing k leads to lower wall-time speedups for both baseline and target methods due to stochastic rejection of tokens, our approach retains its lead achieving better call reduction ratios and walltime speedups across different values of k.

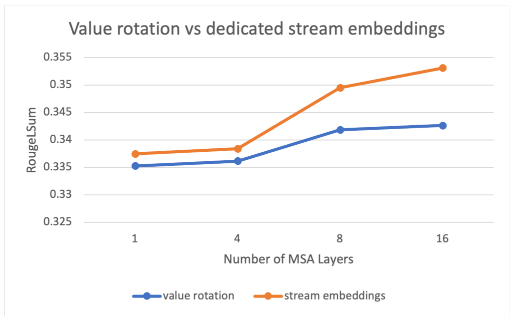

(a)

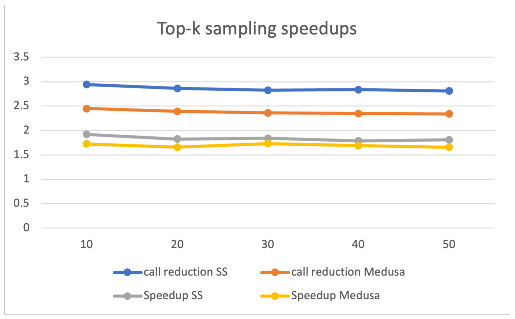

(b)

Figure 11: (a) We analyze the effect of value projection rotation on RougeLSum scores of the Dialog summarization task using PHI-1.3b as the base model for different numbers of MSA layers. Each stream is rotated in proportion to the distance from the main stream. (b) We study the effect of top-k sampling on wall-time speedups and call reduction ratios for Speculative Streaming (SS) and Medusa-style approaches using OPT-1.3b as a base model on the Meaning Representation task.

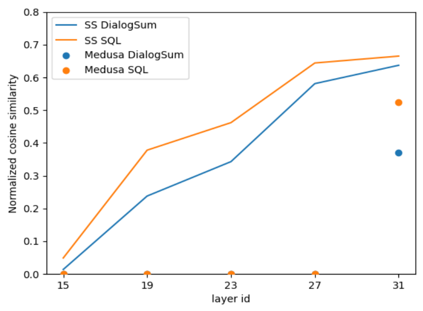

Figure 12: Normalized cosine similarity between speculative residual states and residual state of actual ground truth tokens with Speculative Streaming and Medusa. As the streams propagate through the model, their representations become increasingly aligned with the ground-truth tokens, whereas Medusa speculative residuals are generated from last layer residuals and is less aligned with actual ground truth residuals.

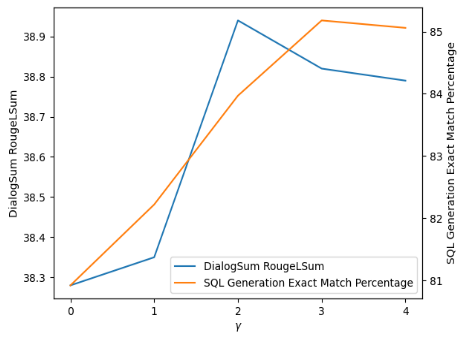

Figure 13: Generation performance of the Phi-3 model when trained to attend to γ ground truth tokens beyond the immediate next token during prediction. The case of $\gamma = 0$ represents the baseline next-token prediction training. Incorporating future ground truth tokens into the attention mechanism leads to substantial improvements in generation performance.

C Segment Attention

Naive training with speculative streaming increases batch dimension along sequence length axis by γ causing attention computation to hit peak memory with larger batches. We propose a segment based attention method that helps reduce peak memory consumption and increases training throughput significantly. We divide each training sample into prompt and multiple segments of completion. Since each stream corresponding to each token needs to attend to it's previous streams of same token and prompt tokens, prompt streams are not required . Moreover, by dividing completion into segments, we just keep streams of current segment in the memory and make them attend to main stream of previously processed segments as depicted in Figure 14.

D Training cost

Since speculative streaming is parameter efficient, training involves fine-tuning only LoRA parameters of MSA layers and it's comparable to training Medusa heads. We finetuned Vicuna-7B model on

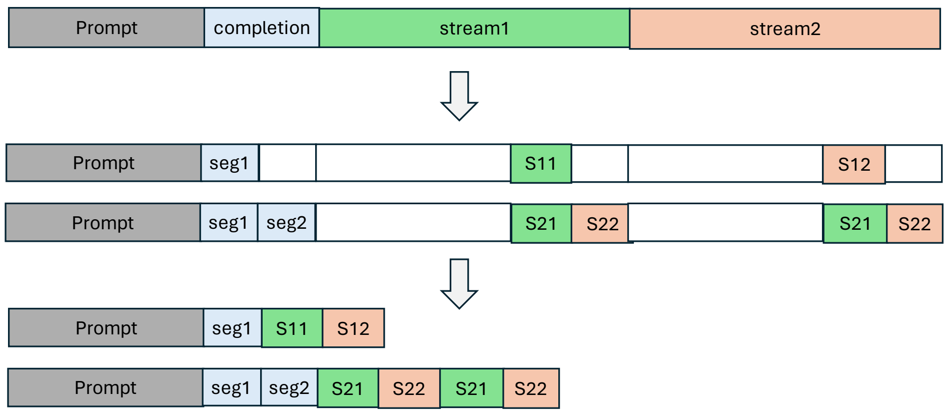

Figure 14: Streams corresponding to prompt are not required while training. Completion is divided into multiple segments and streams of each segment only attend to streams from same segment and main stream of previous segments. Uncolored portion indicates those tokens/streams are not required to be kept in memory. Using segment attention, required peak memory goes down substantially.

the ShareGPT dataset in ~ 5 hours using segment attention, comparable to the 3-4 hours required for training Medusa heads. We also managed to train 33B Vicuna models on a single 80-GB GPU by loading the base model in nf-4 precision and keeping only the adapters of 4 MSA layers in full precision.

E Compute and Memory Profiling

The draft overhead associated with the standard draft-target speculative decoding approach tends to be non-trivial especially when the latency ratio between target and draft models $c_{target}/c_{draft} <= 10$. This is because speculation and verification procedures are run in serial manner. Figure 15 shows the kernel utilization timeline when OPT-125m is used as a draft while OPT-1.3b model is used as the target. Auto-regressive draft generation decreases overall kernel utilization in draft-target approach, while additional computation involved in MSA layers increase kernel utilization in case of Speculative Streaming thereby efficiently utilizing the accelerator and speeding up the decoding process. Negligible cost draft models may offer a better choice to keep kernel utilization at higher levels in case of draft-target approach, however, acceptance rates tend to drop as draft model size decreases.

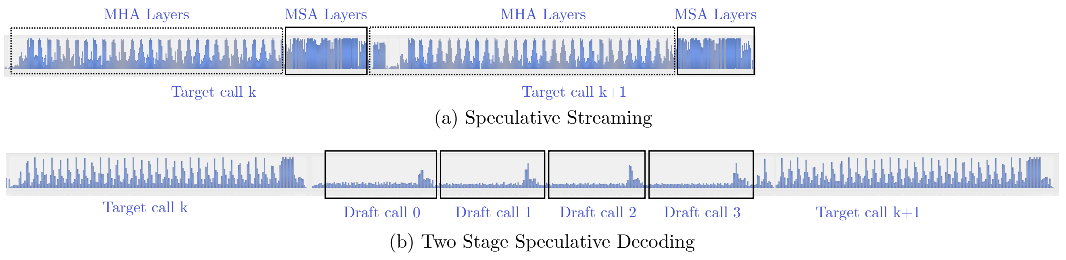

Figure 15: Kernel utilization timeline for speculative streaming and the standard draft-target speculative decoding. Draft-target approach runs speculation and verification in serial manner while it is parallelized in Speculative Streaming. Auto-regressive draft generation often has low kernel utilization as shown leading to decreased overall kernel utilization while MSA layers in Speculative Streaming increase kernel utilization by generating a non-autoregressive draft and speeding up decoding significantly.

F Batching

All the results presented in Section 4 are with batch size of 1 for on-device setup. We also experiment with batching for server setup where queries from multiple users are batched to increase throughput and accelerator utilization. To achieve maximum throughput with batching, we disable tree decoding and tree pruning and use only best speculated path for each decoding step for every sequence in a batch. Since our method primarily relies on utilizing flops to accelerate decoding, with batching we do see some degradation in speedup per sample as depicted in Figure 16, however we consistently achieve >2X speedups while keeping throughput same as batched autoregressive decoding.

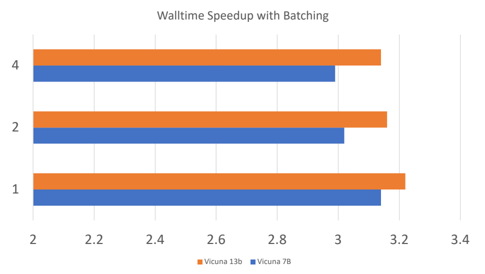

Figure 16: Walltime speedup for different batch sizes with Vicuna Models.

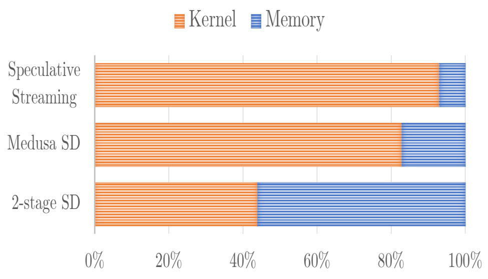

Figure 17: Kernel and Memory utilization comparison on Nvidia A-100.

G Analysis of 2-model speculative decoding

Speculative Streaming consistently achieves significantly lower walltime latency than standard draft-target speculative decoding as depicted in Table 2. It is worth noting that, target model calls of draft-target speculative decoding are slightly lower than Speculative Streaming, however, it comes at the cost of auto-regressively running draft model γ times to generate speculative draft. On the other hand, draft generation with Speculative Streaming incurs almost no additional latency overhead, as target model decoding tends to be memory-bound even with increased tree draft size. This translates to increased kernel utilization and arithmetic intensity as shown in Figure 17.

An argument could be made that a smaller draft model may perform better since drafting should cost less, but acceptance rates may drop as well as the draft model size is decreased. To formalize the comparison with standard draft-target speculative decoding, we do the following analysis, let's say, C_{draft} is the latency cost associated with forward pass through the draft model, C_{target} is the cost associated with forward pass through target model, while C_{ss} is cost associated with speculative streaming forward pass. ζ is the number of decoding tokens advanced during the verification step for the draft-target approach while β is the number of tokens advanced in Speculative Streaming. We equate latency cost associated with single token advancement to compare both approaches.

$$\begin{gathered}(\gamma * C_{draft} + C_{target})/\zeta = C_{ss}/\beta \\ (\gamma + C_{target}/C_{draft})/\zeta = (C_{ss}/C_{draft})/\beta\end{gathered} \tag{10}$$

Assuming $\gamma = 4, C_{target}/C_{draft} = 10$, and $C_{ss} \approx C_{target}$, $\zeta = 1.4\beta$, meaning that advancements per verification step in standard draft-target approach have to be 1.4X of Speculative Streaming to achieve wall time latency parity. Note that, this analysis ignores cache adjustment overhead and prompt processing overhead, but provides valuable intuition to guide the choice between draft-target vs Speculative Streaming approaches. We also analyze under which settings speculative streaming is likely to offer more benefits as compared to the standard draft-target approach. Fig. 1b shows theoretical speedups of Speculative Streaming over draft-target based approach for different Target to draft latency ratios. As the latency ratio increases, the draft-target approach is likely to offer more speedup benefits when $\zeta/\beta > 1$, meaning that when the draft model is accurate enough to achieve more token advancements per target model verification step than Speculative Streaming and also small enough to yield higher latency ratios, it is likely to benefit more. Finding/creating such a model usually requires significant engineering efforts. In downstream application settings, finding ideal draft models becomes even more challenging since ζ tends to vary based on application. If applications share the draft model and only train adapters, the draft model may not remain small enough to meet target-to-draft latency ratios, making it challenging to achieve more speedups than Speculative Streaming.

G.1 Experimental Setup Details

For experiments described in 4, our recipe involves training LoRA adapters for 5 epochs on the downstream datasets in BFloat16, using the AdamQ optimizer, a learning rate of 5e-4, and a linear scheduler. For tree pruning (see Section 3.1.3), we use a low-rank linear transformation of rank 8 to keep parameter overhead minimal. We set $\alpha_0 = 1$ and $\alpha_j = 0.1$ for $j = 1...\gamma$ to weigh speculative loss relative to next token prediction loss. We experimented with linear transformations of different ranks to initialize speculative streams from main stream as described in Equation (3), however we find that simply using identity transformation achieves similar performance with much less parameter overhead. We use identity transformation for all the experiments described in Section 4. We report best results for Medusa and our approach over different γ and k values, while for standard draft-target speculative decoding approach k is fixed to 1. We also report accelerator agnostic speedups (call reduction ratios) assuming negligible verification and draft composition overhead as latency of forward pass, verification and draft composition procedures vary greatly depending on accelerator (a mobile device neural engine Nvidia A100), while call reduction ratio metric tends to serve as roof-line for achievable speedup. Lastly, we use "hard" matching criteria for verification of speculative draft. Relaxing this criteria to "soft" matching may yield higher speedups [5]. To compare with Medusa [5] style approach, we use pre-trained base models with LoRA adapters [16] of rank 32 and Medusa heads as the baseline, and Speculative Streaming with the same base models, stream embeddings and LoRA adapters as target. Medusa heads are trained following the recipe described in [5]. Both Medusa heads and the number of maximum streams are fixed to 4 and the residual blocks per head used in Medusa are set to 1. For comparison with standard draft-target speculative decoding [19], we use OPT models since they come with different configurations and sizes. OPT-125m is deployed as a draft model while OPT-1.3b and OPT-6.7b are used as target models since a ratio of 10-100X is typically considered to be optimal. We compare our approach with LookAhead decoding using best configuration reported in [14].

H Parameter Overhead

In terms of parameters, each Medusa head adds about $h^2 + hv$ parameters, where h is the hidden size and v is the vocabulary size. The number of Medusa heads also scales linearly γ, the length of the speculative window, which in turn increases parameter overhead linearly with γ. On the other hand, Speculative Streaming uses speculative adapters which do not scale with γ. Although, Stream identifier embeddings scale with γ, the parameter overhead associated with each embedding is linear to h. Furthermore, in fine-tuning settings "speculative adapter" parameters are shared with base model adapters, therefore, parameter overhead associated with our approach is just γh.

I Additional Related works

The inference of large language models is often limited by the sequential nature of auto-regressive decoding, where each token generation requires a complete network forward pass. Several approaches have been proposed to address the high inference latency by directly decreasing the memory footprint of LLMs. Model quantization [13, 31, 10], knowledge distillation to a smaller a model [15, 2], and pruning [12, 24] are among these techniques. Recently, speculative decoding (SD) has emerged as a vital technique to accelerate autoregressive decoding.

J Qualitative Examples

In this section, we present qualitative examples to illustrate the effectiveness of Speculative Streaming. By examining specific instances, we aim to highlight how this approach enhances the overall performance of the decoding process. An example of the SQL query generation task is shown in Figure 18, while a dialog summarization example is shown in Figure 19. Each row indicates the

SELECT in _ count y

SELECT in _ count y _ tu ition _ per

SELECT in _ count y _ tu ition _ per_ credit _ ~~credit _~~

SELECT in _ count y _ tu ition _ per_ credit _ hour __ fall _ ~~_~~

SELECT in _ count y _ tu ition _ per_ credit _ hour __ fall _ 2009 _ FROM table _

SELECT in _ count y _ tu ition _ per_ credit _ hour __ fall _ 2009 _ FROM table _ 22 30 88 81 _

SELECT in _ count y _ tu ition _ per_ credit _ hour __ fall _ 2009 _ FROM table _ 22 30 88 81 _ 2 WHERE college = "

SELECT in _ count y _ tu ition _ per_ credit _ hour __ fall _ 2009 _ FROM table _ 22 30 88 81 _ 2 WHERE college = " Mer ~~Er " College <\s>~~

SELECT in _ count y _ tu ition _ per_ credit _ hour __ fall _ 2009 _ FROM table _ 22 30 88 81 _ 2 WHERE college = " Mer Cer " <\s>

Figure 18: Speculative streaming on SQL generation task for $\gamma = 4$ and $k = 1$, each pass verifies the previous draft and generates a maximum of 5 tokens. For instance in pass 4, "$credit$" and "_" (shown in red) are rejected and "$hour$", "_", "$fall$", "_", "_" are speculated.

# Person 2 # ~~and~~

# Person 2 # thinks Lincoln ~~is a character~~

# Person 2 # thinks Lincoln was a ~~character and he~~

# Person 2 # thinks Lincoln was a man of ~~character and he~~

# Person 2 # thinks Lincoln was a man of sound character and # person

# Person 2 # thinks Lincoln was a man of sound character and # person 1 # adm ires him

# Person 2 # thinks Lincoln was a man of sound character and # person 1 # adm ires him for his courage and ~~and~~

# Person 2 # thinks Lincoln was a man of sound character and # person 1 # adm ires him for his courage and rights and humility . </s>

Figure 19: Speculative streaming on Dialog Summarization task for $\gamma = 4$ and $k = 1$, each pass verifies the previous draft and generates a maximum of 5 tokens. For instance, in pass 3, "is", "a", "$character$" are rejected and "was", "a", "$character$", "and", "he" are speculated.

previous sequence of accepted draft tokens (in black) and the new sequence of generated tokens in green/red. We use $\gamma = 4$ and $k = 1$ to illustrate the decoding process. Green tokens in each row indicate tokens accepted in the next forward pass, while red tokens indicate tokens rejected in the next forward pass. Speculative Streaming appears to generate meaningful drafts with high acceptance rates by capturing dependencies between tokens quite effectively, despite generating them in a non-auto-regressive manner.